Analysis of Periodic Growth–Disturbance Models

Timothy C. Reluga

treluga@amath.washington.edu

Department of Applied Mathematics

University of Washington

Seattle, WA 98195

October 16, 2004

Running title: Growth–Disturbance Models

Key words: periodic disturbance, period-bubbling, seed bank, density dependence, population ecology

Abstract

In this paper, I present and discuss a potentially useful modeling approach for investigating population dynamics in the presence of disturbance. Using the motivating example of wildfire, I construct and analyze a deterministic model of population dynamics with periodic disturbances independent of spatial effects. Plant population growth is coupled to fire disturbance to create a growth–disturbance model for a fluctuating population. Changes in the disturbance frequency are shown to generate a period-bubbling bifurcation structure and population dynamics that are most variable at intermediate disturbance frequencies. Similar dynamics are observed when the model is extended to include a seed bank. Some general conditions necessary for a rich bifurcation structure in growth–disturbance models are discussed.

1 Introduction

In ecology, disturbances are irregular and infrequent events that significantly alter systems relative to their pre-disturbance states (Sousa, 1984). Biological disturbances, which are traditionally destructive and may include forest fires, volcanic eruptions, and hurricanes, occur quickly, perhaps over a period of hours. Yet, the disturbed systems may take years to recover.

Ecologists have been aware of the importance of disturbance since the inception of the field in the late 1800's. In an early work, Ernst (1908) summarized the succession of flora on Krakatau's neighboring islands following the 1883 eruption. A large body of literature on disturbance in populations and ecosystems has accumulated in the succeeding years (Pickett and White, 1985; Sousa, 1984). Clements (1916) developed the concept of ecological succession around disturbances like forest fires. Andrewartha and Birch (1978) proposed that disturbances and temporal heterogeneity, particularly in the form of weather events, were responsible for all population regulation. Hutchinson (1961) argued that disturbances were essential for maintaining biodiversity in plankton communities. More recently, disturbance has been central in non-equilibrium theory (Sommer and Worm, 2002) and metapopulation theory (Hanski, 1999). Disturbance also plays an important if controversial (Mackey and Currie, 2000; Hastwell, 2001) role in biodiversity theory through neutral models (Hubbell, 2001) and the Intermediate Disturbance Hypothesis (Grime, 1973; Connell, 1978). These theories have had mixed success. A century of research have shown that disturbance has different flavors (trophic and environmental) and different textures (from individual scales to global scales) (Sheil and Burslem, 2003).

Mathematical models may help us understand disturbance, but development of a mathematical theory of population disturbance has lagged behind empirical studies. Early works on impulsively forced population models include the rabies model of (Bartoszynski, 1975) and the disaster model of Kaplan et al. (1975), but the first modern model to explicitly incorporate disturbance was developed by Hanson and Tuckwell (1978). Hanson and Tuckwell used stochastic processes to study extinction rates in populations experiencing logistic growth and discrete shocks of fixed magnitude whose times were drawn from a Poisson process. Their work has been generalized

in various papers (Brockwell, 1986; Lande, 1993; Hanson and Tuckwell, 1997). A practical approach to modeling disturbance has been presented by Silva et al. (1991) and is based on the use of stochastic matrix models to describe asymptotic growth rates. This approach has been improved by Caswell and Kaye (Caswell and Kaye, 2001; Caswell, 2001) and others. The earliest theoretic work concerning catastrophic disturbance in multi-species models appears to be that of Huston (1979). Huston argued that disturbance can slow processes of competitive exclusion. Huston's qualitative results have been expanded to include trophic structure by Wootton (1998).

Contemporary models incorporating disturbance range from deterministic, time-averaged, spatially-implicit models (Hanski, 1999) to stochastic, individual-based, spatially-explicit simulation models (McGlade, 1999). An important intermediate class of models consists of deterministic, spatially-implicit models explicitly incorporating periodic disturbance. This class of models is useful for distinguishing effects that are consequences of general nonlinear interactions from those effects that are fundamentally spatial or stochastic consequences of disturbance.

Surprisingly, only a few models have addressed periodic disturbance in the absence of spatial and stochastic effects. These models have usually considered disturbance functions that alter the population size by a constant number of individuals or a constant fraction of current population size. Ives et al. (2000), for instance, studied the effects of disturbance proportional to population size on a Lotka–Volterra model with prey density dependence. Related work by Liu and Chen (2003) analyzes the Rosenzweig–MacArthur predator–prey model in the presence of periodic immigration of a constant number of predators. Chau (2000) discusses the dynamics, under periodic harvesting of a fixed number of individuals, in Ricker (Ricker, 1954) and Nicholson–Bailey (Nicholson and Bailey, 1935) models. Grant et al. (1997) present some simulation examples of logistic growth and multi-species competition under periodic removal of a fixed fraction of the population, but do not perform a systematic analysis or provide references. A few works consider periodic density-dependent disturbance. Grant et al. (1997), for instance, simulate biomass accumulation subject to a fire management strategy that subjects the populations to nonlinear disturbance, and Bascompte and Rodriguez (2000) consider nonlinear disturbance from biomass accumulation in tallgrass prairies using a difference-equation model.

The purpose of this paper is two-fold. First, it formalizes a pre-existing but poorly developed framework, referred to as growth–disturbance modeling, for the analysis of population dynamics in the presence of periodic disturbance. This approach, a simplification of that used by Hanson and Tuckwell (1978), is a natural starting point for many investigations. Second, this paper illustrates the potential usefulness of growth–disturbance models by analyzing two simple models in which both growth and disturbance are nonlinear functions of population density. These models are motivated by the example of wildfire disturbance, where there is a complex relationship between fuel, fire intensity, and population dynamics.

This paper presents and analyzes the dynamics of a population under periodic disturbance in both a scalar and two-stage model. First, it presents a thorough analysis of a scalar model that combines disturbance with exponential or logistic growth in the context of wildfire (Section 2). This model serves as an archetype. The carrying capacity of logistic growth stabilizes dynamics when compared with exponential growth. Varying the disturbance frequency generates a period-bubbling bifurcation structure (Bier and Bountis, 1984; Stone, 1993). The scalar model is then expanded (Section 3) to a two-stage model by inclusion of a seed bank. I describe a general approach for analysis of models without closed-form solutions and show that the dynamics of the two-stage model are similar to those of the scalar model for parameter regimes where both stages experience significant fire mortality. The paper closes with a discussion of necessary conditions for the observed bifurcation structures in the context of growth–disturbance models.

2 Growth–Disturbance in Scalar Models

Growth–disturbance models are convenient when researchers, who have already developed a growth model, wish to investigate the effects of disturbance on this model. Growth–disturbance models assume that disturbances happen quickly and that factors governing population growth under normal circumstances are temporarily irrelevant during a disturbance. Under these circumstances, a completely independent model is constructed to describe the response to disturbance. By coupling the independent models for growth and disturbance, we derive a mapping that is well-suited to the

study of a population's long-term dynamics. Growth–disturbance models appear elsewhere in the theoretical biology literature (Ives et al., 2000; Roberts and Heesterbeek, 1998), though not under this name.

The modeling approach is general, but I will use the motivating example of wildfire in the subsequent formulation and analysis. A localized, spatially homogeneous population of woody shrubs experiences periodic fires. Between fires, the population exhibits deterministic growth,

$$\frac{dN}{dT} = rf(N)N, \tag{1}$$

where T is time, N is the population's size, and $rf(N)$ is the population's per capita rate of growth.

Every few years, a fire burns through the population. In general, a shrub population will burn sporadically, and the timing of the fire regime is described by a stochastic process. As a mathematical convenience for studying dynamics, I postulate that wildfires recur deterministically with fixed period τ. These fires will cause periodic crashes in the population that must be governed by a separate "jump" condition

$$N_+ = S(N_-)N_-, \tag{2}$$

where N_- is the size of the population immediately preceding a fire, N_+ is the size of the population immediately following a fire, and $S(N_-)$ is the fire survivorship. Eqs. (1) and (2) form the general framework for growth–disturbance models and are summarized in Fig. 1. In the mathematical literature, they correspond to an "impulsive differential equation" (Bainov and Simeonov, 1993). For coupled populations, N is a vector, $rf(N)$ is a matrix, and $S(N_-)$ is a positive, diagonal matrix, but I will restrict myself to the scalar case for the moment.

The choice of a disturbance survivorship $S(N_-)$ is a central issue in growth–disturbance modeling. In the simplest case, where the effects of disturbance on every individual are independent of one another, it is reasonable to assume

$$\frac{dS(N_-)}{dN_-} = 0\,, \tag{3}$$

leading to constant survivorship. In the case of the Lotka–Volterra predator–prey equations, Ives et al. (2000) showed that periodic linear disturbance can lead to novel and unexpected dynamics.

When survivorship is controlled exogenously, perhaps by harvesting, mortality may be independent of population size so that

$$S(N_-) = \max\{0, 1 - \frac{m}{N_-}\} \, . \tag{4}$$

This is similar to the form used by Chau (2000) and implicitly by Stone (1993). Both of these works showed that immigration stabilized dynamics ($m < 0$), but the results for disturbance ($m > 0$) were less clear.

Here, I will investigate a general class of nonlinear survivorships. If the size of the disturbance-induced crash is controlled by the strength of the fire and the predominant form of fire fuel is shrub biomass (generating an instantaneous form of density-dependent feedback), survivorship can be assumed to take the form

$$S(N) = \frac{1}{1 + (AN)^{\beta}}, \tag{5}$$

where A is a constant of proportionality, with units of fuel loading per individual, and β is a nonlinear shape parameter. This functional form, henceforth referred to as the generalized Beverton–Holt form, was introduced into ecology by Maynard Smith and Slatkin (1973) to describe density dependent population growth and was promoted by Bellows (1981) over the more common Hassell (1975) and Ricker (1954) model formulations. The generalized Beverton–Holt equation's behavior is well understood, and has been analyzed by Doebeli (1995) and Getz (1996) among others. Small β corresponds to fire effects with weak density dependence. For large β, Eq. 5 exhibits threshold behavior typical of percolation-driven phenomena like fire, with high survivorship for low densities ($N < 1/A$), and low survivorship for high densities ($N > 1/A$). As $\beta \to \infty$, the survivorship may exhibit an arbitrarily thin algebraic tail. To maintain consistency with the percolation analogy, I have also chosen Eq. 5 so that the survivorship approaches 1 for small populations. This prevents extinction, which has been studied elsewhere (Brockwell, 1986; Gripenberg, 1985), and allows this work to focus on dynamics.

Using the survivorship described by Eq. (5), N_- and N_+ satisfy the jump condition

$$N_+ = \frac{N_-}{1 + A^{\beta} N_-^{\beta}}. \tag{6}$$

The growth and disturbance equations, Eqs. (1) and (6), are transformed to dimensionless form by $x = AN$ and $t = rT$, so that

$$\dot{x} = x f(x/A), \tag{7}$$

$$x_+ = \frac{x_-}{1 + x_-^{\beta}}, \tag{8}$$

where Eq. (8) is applied every τ time units.

For comparison, two different cases for the per capita growth rate $f(x/A)$ are considered: density independence and simple density dependence. Under density independence, with $f(x/A) \equiv 1$,

$$\dot{x} = x. \tag{9}$$

Eq. (9) has the solution $x = x_0 e^t$, in terms of the initial population x_0 and time t. With this solution, Eqs. (7) and (8) reduce to a stroboscopic mapping that relates population size immediately after one fire to the population size immediately after the next fire, τ time units later (see Fig. 2):

$$x_{n+1} = \frac{x_n e^{\tau}}{1 + (x_n e^{\tau})^{\beta}} \equiv g(x_n). \tag{10}$$

Alternatively, limited resource availability may introduce density-dependent pressures corresponding to logistic growth:

$$f(y) \equiv \frac{K - y}{K}. \tag{11}$$

The growth rate is now

$$\dot{x} = x\left(\frac{K - x/A}{K}\right) = x\left(\frac{\kappa - x}{\kappa}\right), \tag{12}$$

where $\kappa = KA$. Paralleling the argument of the preceding paragraph, when disturbances occur with fixed period τ, the associated stroboscopic mapping is (see Fig. 2)

$$\begin{aligned} x_{n+1} =& \frac{x_n \kappa e^{\tau}}{x_n e^{\tau} + \kappa - x_n} \left[1 + \left(\frac{x_n \kappa e^{\tau}}{x_n e^{\tau} + \kappa - x_n}\right)^{\beta}\right]^{-1} \\ =& \frac{\kappa x_n \left[x_n + (\kappa - x_n) e^{-\tau}\right]^{\beta - 1}}{\left[x_n + (\kappa - x_n) e^{-\tau}\right]^{\beta} + (\kappa x_n)^{\beta}} \equiv h(x_n). \end{aligned} \tag{13}$$

Stroboscopic mappings like (10) and (13) are central to the analysis of growth–disturbance models. These stroboscopic mappings, in concert with the integrated growth equations, completely

determine a population's time evolution. The stroboscopic mapping's solution reveals the population size after each disturbance. Given a solution to a stroboscopic mapping, the population level at any intermediate time can be determined by integrating the growth model with initial conditions obtained from the mapping's solution.

2.1 Analysis of the Stroboscopic mappings

Eq. (10), which describes disturbance in the presence of exponential growth, is a generalized version of the Beverton–Holt equation (Beverton and Holt, 1956). The function $g(x)$ vanishes at $x = 0$, has a maximum at

$$x = e^{-\tau}/(\beta - 1)^{1/\beta} \tag{14}$$

for $\beta > 1$, and approaches 0 as x grows, for $\beta > 1$ (see Fig. 2). A unique positive fixed point $x^* = g(x^*)$ occurs at $x^* = (e^{\tau} - 1)^{1/\beta} e^{-\tau}$. The slope at x^* is $1 - \beta + \beta e^{-\tau}$ and it follows that x^* is stable only if

$$\beta < \frac{2}{1 - e^{-\tau}}. \tag{15}$$

For large τ, the slope at x^* is approximately $1 - \beta$, so x^* must be stable if $0 < \beta < 2$. It can be shown numerically that Eq. (10) exhibits a period-doubling route to chaos for large β and τ (see Fig. 3).

Eq. (13), which describes disturbance with logistic growth, is equivalent to Eq. (10) in the $\kappa \to \infty$ limit. For finite κ, $h(x)$ has a finite limit for large x:

$$\lim_{x \to \infty} h(x) = \frac{\kappa(1 - e^{-\tau})^{\beta - 1}}{\kappa^{\beta} + (1 - e^{-\tau})^{\beta}}. \tag{16}$$

When $(\beta - 1)^{1/\beta} < (1 - e^{-\tau})/k$, $h(x)$ monotonically increases from 0 to this asymptote. When $(\beta - 1)^{1/\beta} > (1 - e^{-\tau})/k$, $h(x)$ first increases from 0 to a maximum at

$$x = \frac{\kappa}{1 - e^{\tau} + \kappa e^{\tau}(\beta - 1)^{1/\beta}}, \; h(x) = \frac{(b - 1)^{1 - 1/b}}{b} \tag{17}$$

before monotonically decaying to the horizontal asymptote (see Fig. 2). There is no simple closed-form solution for the steady-state $x^* = h(x^*)$, but qualitative arguments can be used to show that the steady-state equation has a unique positive solution.

For τ and κ fixed and $\beta \to \infty$, Eq. (13) exhibits the classic period-doubling route to chaos (see Fig. 4), but for β and κ fixed and β sufficiently large, Eq. (13) exhibits period-bubbling (Bier and Bountis, 1984; Stone, 1993) in τ (see Figs. 3 and 5). For period-bubbling, the regular bifurcation pattern reverses itself, undergoes period halving via flip bifurcations, and eventually returns to a unique steady-state for large parameter values. The presence of period-bubbling is the major difference between the density-independent and density-dependent growth models.

In scalar mappings, flip bifurcations occur when parameter changes drive the slope at a fixed point below -1. To locate a flip bifurcation, we need to simultaneously solve $h(x) = x$ and $h'(x) = -1$. In our case,

$$\frac{\kappa x\left[x+(\kappa-x)\,e^{-\tau}\right]^{\beta-1}}{\left[x+(\kappa-x)\,e^{-\tau}\right]^{\beta}+(\kappa x)^{\beta}} = x \tag{18}$$

and

$$\frac{\kappa^2 e^{-\tau}\left[x+(\kappa-x)\,e^{-\tau}\right]^{\beta-2}\left\{\left[x+(\kappa-x)\,e^{-\tau}\right]^{\beta}-(\beta-1)\,(\kappa x)^{\beta}\right\}}{\left\{\left[x+(\kappa-x)\,e^{-\tau}\right]^{\beta}+(\kappa x)^{\beta}\right\}^{2}} = -1. \tag{19}$$

From Eqs. (18) and (19), we can show that the flip bifurcations of mapping (13) occur for parameter values satisfying

$$\left[\frac{(\beta-1)(e^{\tau}-1)}{\kappa(\beta e^{\tau}-\beta-2e^{\tau})}\right]^{\beta} = \frac{\beta-1}{e^{\tau}+1} \tag{20}$$

(see Fig. 6). Asymptotic analysis of Eq. (20) as $\beta \to \infty$ (see Appendix A) shows that the region of bubbling has approximate boundaries

$$\frac{2\kappa}{\beta(\kappa-1)} < \tau < \beta\ln\kappa+\ln\beta-1. \tag{21}$$

To highest order in β, the size of the region of period-bubbling grows linearly with β, and logarithmically in κ.

Though Eqs. (10) and (13) depend nonlinearly upon their parameters, the observed dynamics can be directly related to the biological roles of β, κ, and τ. The shape parameter β has straightforward effects: the stability near the rest point increases and the variability of x_n declines as β decreases. A comparison of dynamics for the exponential growth and logistic growth shows that the density dependence introduced by κ has a stabilizing effect. When there exists a finite carrying

capacity and the time between disturbances is sufficiently large, a population will approach carrying capacity and exhibit little time variation in x_n when compared with an exponentially growing population.

The role of the disturbance period τ is the most complex of the three parameters. If either β or κ is sufficiently small, the system is attracted to a global steady-state for all τ. If both β and κ are larger, one finds four distinct regions of behavior in the density-dependent model (Fig. 5). At very high disturbance rates (small τ), there is a boundary layer in which the population can be driven to arbitrary low levels. Except for this boundary layer, the minimum observed population level declines(to first order) toward $h(\infty)$ as τ increases. At moderately high disturbance rates, the population will persist at relatively high levels. At intermediate disturbance rates, the dynamics become chaotic and the greatest fluctuations are observed. At very low disturbance rates, variability in the stroboscopic mapping is lost, and the population will spend most of its time near carrying capacity with the exception of rare crashes down to $h(\infty)$. Thus, increasing the fire frequency can either increase or decrease stability, depending upon the values of the other parameters, κ and β.

In summary, we see that the scalar growth–disturbance model has a unique positive fixed point in both the exponential growth and logistic growth cases, Eqs. (10) and (13) respectively. In the case of exponential growth, the positive steady-state becomes less stable as the time between disturbances grows, but in the case of logistic growth, saturation effects stabilize the fixed point when the disturbance period is very long. As will be shown in the next section, this pattern may also occur in a 2-stage model.

3 A Two-Stage Model

When population models are extended to include population structure, the relationship between growth and disturbance becomes more complex. Parameters proliferate on the order of the square of the system dimension, and the ordinary differential equations describing growth rarely have closed-form solutions. As a consequence, general analytic results similar to those of the previ-

ous section are rarely available. Instead, we must augment the occasional asymptotic result with numerical experiments. As a final example, I consider an extension of the scalar model of fire disturbance, Eqs. (7) and (8), to include a seed bank stage, and describe the application of the growth–disturbance method from a numerical perspective. This example shows the rich bifurcation structures of the previous example is not universal and suggests that singular phase-space orbits are important in the generation of these structures.

Consider an ideal plant population with 2 stages: seed bank and adult. Under the simplest assumptions, seeds are produced at a rate proportional to the adult population, $N_2(T)$, but sprout at a rate proportional to the number of seeds, $N_1(T)$, present. Adults die at a rate proportional to their abundance and are replaced by sprouting seeds. The success of sprouting seeds, however, is limited by competition from the adult population. Thus,

$$\begin{bmatrix} \frac{dN_1}{dT} \\ \frac{dN_2}{dT} \end{bmatrix} = \begin{bmatrix} -a & R \\ a\left(1-\frac{R-m}{RK}N_2\right) & -m \end{bmatrix} \begin{bmatrix} N_1 \\ N_2 \end{bmatrix} \tag{22}$$

where R is the rate of seed production per adult, K is the adult carrying capacity, m is the adult mortality rate, and a is the sprouting rate of seeds. This nonlinear model, loosely related to one developed by Aiello and Freedman (1990), is an exception to standard stage-structured models. There is no seasonal or developmental delay present. Stage-structured models without delays are roughly valid for large populations under ideal growing conditions, where turnover rates are small, and juvenile development is rapid relative to adult life expectancy.

When incorporating disturbance by fire within a structured population model, different stages contribute differently to fuel levels and have different fire-tolerance levels. Adopting the generalized Beverton-Holt form discussed in Section 2, the survivorship of the i'th stage may be described in terms of the accumulated fuel as

$$N_{i+} = \frac{N_{i-}}{1+\left(A_i \sum_{\forall j} I_j N_{j-}\right)^{\beta_i}}, \tag{23}$$

where I_j is the fuel contribution per individual of the j'th stage, and A_i and β_i describe the saturation behavior for the i'th stage. As in Section 2, these disturbance functions postulate that the survivorship is approximately 1 when the population is small.

To reduce the parameter space, I will make the additional assumption that seeds do not contribute to fuel loading ($I_1 = 0$). Thus, for the seed bank model,

$$N_{1+} = \frac{N_{1-}}{1 + (A_1 I_2 N_{2-})^{\beta_1}}, \tag{24}$$

$$N_{2+} = \frac{N_{2-}}{1 + (A_2 I_2 N_{2-})^{\beta_2}}. \tag{25}$$

Performing the transformation

$$t = aT, \tag{26}$$

and the reparameterizations

$$x = N_1,\ y = A_2 I_2 N_2,\ \gamma = \frac{A_1}{A_2},\ \rho = \frac{R}{a A_2 I_2},\ \mu = \frac{m}{a A_2 I_2},\ \kappa = k A_2 I_2, \tag{27}$$

we obtain the dimensionless formulation

$$\dot{x} = -x + \rho y, \tag{28}$$

$$\dot{y} = x\left(1 - \frac{\rho - \mu}{\rho\kappa} y\right) - \mu y. \tag{29}$$

$$x_+ = \frac{x_-}{1 + (\gamma y_-)^{\beta_1}}, \tag{30}$$

$$y_+ = \frac{y_-}{1 + y_-^{\beta_2}}. \tag{31}$$

The previous assumption that disturbance recurs with fixed period τ still holds.

The seed bank model growth equations, Eqs. (28) and (29), have steady-states

$$\left(x_{eq}, y_{eq}\right) \in \left\{(0,0), (\rho\kappa, \kappa)\right\}. \tag{32}$$

As long as $\rho > \mu$, the positive equilibrium is an attracting node and the global attractor of the invariant first quadrant. Unlike the scalar case considered previously, the seed bank growth equations lack a closed-form solution. Instead, they must be integrated numerically. For an arbitrary differential equation, the numerical integrator should be chosen with care, but for many biological models, a 4th order Runge–Kutta–Fehlberg method has historically been adequate. Growth–disturbance models treat numerically integrated solutions the same as closed-form solutions. From an initial condition, we first integrate the growth model's equations τ time units forward to determine the

population levels just prior to the next disturbance. The disturbance model is then applied. The disturbance model yields the initial conditions for the next integration of the growth model, and the process repeats.

The solution of Eqs. (28) and (29) given initial conditions (x_0, y_0) and time t may be represented as a pair of functions

$$[x(t), y(t)] = [g_x(t, x_0, y_0),\ g_y(t, x_0, y_0)]\ , \tag{33}$$

where $g_x()$ and $g_y()$ denote the results of the numerical integration procedure. Employing the above representation, one need only study the mappings

$$x_{n+1} = \frac{g_x(\tau, x_n, y_n)}{1 + [\gamma g_y(\tau, x_n, y_n)]^{\beta_1}}\ , \tag{34}$$

$$y_{n+1} = \frac{g_y(\tau, x_n, y_n)}{1 + [g_y(\tau, x_n, y_n)]^{\beta_2}}\ . \tag{35}$$

It is conjectured that Eqs. (34) and (35) have a unique positive fixed point for all feasible parameter values. Although quantitative results are difficult to obtain, we may easily observe certain qualitative properties in the dynamics of Eqs. (34) and (35) under numerical iteration.

For some parameter regimes, the seed bank extension exhibits a τ bifurcation structure very similar to that of the scalar model (compare Figs. 7 and 5). When β_1 and β_2 are large, the mapping's positive fixed point may become unstable for intermediate τ. When τ is large or small, or $\kappa < \max(1, 1/\gamma)$, the positive fixed point is stable.

However, there are some parameter regimes where the stability of the fixed point is extremely robust, and only very weak bifurcation structures can be observed. Specifically, consider the situation where seeds are immune to fire ($\gamma = 0$). In this special case, Eqs. (34) and (35) reduce to

$$x_{n+1} = g_x(t, x_n, y_n) \tag{36}$$

$$y_{n+1} = \frac{g_y(t, x_n, y_n)}{1 + [g_y(\tau, x_n, y_n)]^{\beta_2}}. \tag{37}$$

The reduced mappings (36) and (37) have far less eccentric behavior than the full mappings described by (34) and (35). When all other relevant parameters are comparable, the reduced mappings' positive fixed point is stable for larger β values than the full mappings' positive fixed point.

Even when the reduced mappings exhibit instability, the bifurcation diagrams never exhibit the complexity of Fig. 7. In short, the reduced mappings (36) and (37) are less variable than the full mappings (34) and (35).

The dramatic differences in behavior between these two cases are attributable to the role of singular phase-space orbits in the underlying differential equations. In the full stroboscopic mappings (34) and (35), disturbance drives the solution of the differential equation toward the singular orbit $(0,0)$. Since the differential equation changes slowly in the neighborhood of this point, timescales become stretched, accentuating small perturbations and producing richer dynamics. In the reduced stroboscopic mappings (36) and (37), disturbance drives the initial condition toward the x axis, but NOT toward the origin since the x value is unaffected by disturbance. Eqs. (28) and (29) do not exhibit any singular behavior along the x axis away from the origin. Even if all adults are instantly killed off, much of the short-term reproductive potential of the population remains in the seed bank. Solutions move away from the x axis with finite speed, so that increasing the severity of disturbance has little effect on the evolution of the differential equations describing growth. Thus, the reduced mappings (36) and (37) may be expected to have calmer asymptotic dynamics than the full mappings (34) and (35).

4 Discussion

In this paper, I have described a general approach for extending ordinary differential equation models to include nonlinear disturbance. As the motivating example, a model of a plant population under periodic disturbance by wildfire has been presented. The resulting growth–disturbance models are caricatures of biological reality but preserve several biologically significant features.

The behavior of the scalar model presented in Section 2 is dependent upon three dimensionless parameters: disturbance period, carrying capacity, and disturbance nonlinearity. In dimensional variables, the first two parameters correspond to the ratio of disturbance period to population doubling time and the ratio of carrying capacity to the disturbance half-saturation level. As summarized by Fig. 6, the regions of parameter space for which the stroboscopic steady-state is stable

grow as the dimensionless carrying capacity or the disturbance nonlinearity decrease. In contrast, the variability of the response to disturbance is a unimodal function of the disturbance period. Similar behaviors are numerically observed in the stage structured seed bank model for parameter sets where both adults and seeds can suffer heavy fire mortality.

The primary observation to be emphasized is that, in the presence of a carrying capacity, the response to disturbance is most variable at intermediate disturbance rates and least variable for high and low disturbance rates. This is observed in both examples with nonlinear growth, but not in the scalar model incorporating exponential growth. Although not presented here, it is possible to prove that the unimodal dependence on disturbance period holds for a large class of stage-structured growth equations with a globally attracting steady-state. This peaked response in variability strongly resembles results from a spatially explicit disturbance simulation performed by Turner et al. (1993). Similar stability results in the context of delayed nonlinear feedback were obtained by Bascompte and Rodriguez (2000) with regards to grassland self-disturbance and by Hastings and Constantino (1987) with regards to cannibalism. If this relationship extends to models with many interacting species, it suggests a connection to the Intermediate Disturbance Hypothesis (Grime, 1973; Connell, 1978; Wilkinson, 1999) that deserves further investigation. At the same time, it must be said that density-dependent growth is only one of several phenomena that may generate unimodal variability. It is relatively easy, for instance, to construct a disturbance function for a scalar model with exponential population growth that also exhibits period-bubbling. A comprehensive survey of scalar growth–disturbance models would be useful in characterizing the potential mechanisms of period-bubbling, but is currently unavailable.

As the analysis of the seed bank extension in Section 3 demonstrates, the complex bifurcation structures seen in Fig. 5 are not universal, but are more likely to arise when the “direction” of disturbance brings the solution near an unstable steady-state of the growth sub-model. This suggests the existence of a spectrum of biological response to disturbance. At one extreme, populations are “well”-adjusted to disturbance and recovery occurs in an orderly fashion. At the other extreme, populations are “ill”-adjusted to disturbance and the recovery path is indeterminate. In cases where the populations are “ill”-adjusted, the nature of the instabilities suggests the recovery path will be

sensitive to small stochastic effects.

Two other general but less significant phenomena are observed. First, as the degree of disturbance nonlinearity increases, the dynamics of growth–disturbance models become more complex. Second, the reduction of carrying capacities can stabilize the dynamics of a population under periodic disturbance. This is most obvious in the analysis of the scalar model in Section 2 but is also present in the seed bank model. In Eq. (21), the region of instability grows according to $\ln \kappa$, a quantity which also arises in the classical sensitivity results of Southwood (1976) and Rosenzweig (1971).

Growth–disturbance models appear to be a useful theoretical tool. Hopefully, they will also be a useful practical tool. Directions for future work include a systematic classification of scalar models, relaxation of the periodicity constraint on disturbance, incorporation of delay differential equation growth models, and application to models with more complex stage-structure.

Acknowledgments

The author would like to thank Mark Kot and two anonymous reviewers for their constructive comments. This work was supported by NSF VIGRE grant DMS-9810726.

A Asymptotic Bounds on Period Bubbling in the Scalar Model

To obtain asymptotic bounds on the region of period bubbling from Eq. (21), start with Eq. (20)

$$\left[\frac{(\beta-1)(e^{\tau}-1)}{k(\beta e^{\tau}-\beta-2e^{\tau})}\right]^{\beta}=\frac{\beta-1}{e^{\tau}+1}. \tag{38}$$

There are two solution branches as $\beta\to\infty$: a lower branch where τ is bounded, and a upper branch where $\tau\to\infty$. Consider the upper branch first. As $\tau\to\infty$, terms that are exponential in τ dominate constant and algebraic terms,

$$\left[\frac{(\beta-1)e^{\tau}}{k(\beta e^{\tau}-2e^{\tau})}\right]^{\beta}\sim\frac{\beta-1}{e^{\tau}}. \tag{39}$$

Taking reciprocals and canceling common factors,

$$\left[\frac{k(\beta-2)}{\beta-1}\right]^{\beta}\sim\frac{e^{\tau}}{\beta-1}. \tag{40}$$

Taking logarithms and utilizing a Taylor series expansion,

$$\tau\sim\beta\ln k+\ln\beta-1-\frac{5}{2\beta}+o(\beta^{-1}). \tag{41}$$

A little more care is needed to find the lower branch. Consider $\beta\to\infty$, τ and κ bounded, and $\kappa>1$. Inspection of Eq. (38) suggests that the left hand side grows exponentially unless it is equal to 1 to first order. Since τ is bounded, the right hand side can not grow exponentially, only algebraically. This implies the zeroth-order matching condition

$$\left[\frac{(\beta-1)(e^{\tau}-1)}{k(\beta e^{\tau}-\beta-2e^{\tau})}\right]^{\beta}\sim 1. \tag{42}$$

Taking the β'th root,

$$\frac{(\beta-1)(e^{\tau}-1)}{k(\beta e^{\tau}-\beta-2e^{\tau})}\sim 1. \tag{43}$$

Solving for τ and using asymptotic expansions, we conclude

$$\tau \sim \frac{2\kappa}{\beta(\kappa-1)} + o(\beta^{-1}). \tag{44}$$

References

Aiello, W. G., Freedman, H. I., 1990. A time-delay model of single-species growth with stage structure. Mathematical Biosciences 101, 139–153.

Andrewartha, H. G., Birch, L. C., 1978. A general theory on the numbers of animals in natural populations. In: Tamarin, R. H. (Ed.), Population Regulation. Vol. 7 of Benchmark Papers in Ecology. Dowden, Hutchinson, and Ross, Stroudsburg, PA, pp. 73–90.

Bainov, D., Simeonov, P., 1993. Impulsively Differential Equations: Periodic Solutions and Applications. Longman, Essex, UK.

Bartoszynski, R., 1975. On the risk of rabies. Mathematical Biosciences 24, 355–377.

Bascompte, J., Rodriguez, M. A., 2000. Self-disturbance as a source of spatiotemporal heterogeneity: the case of the tallgrasss prairie. Journal of Theoretical Biology 204, 153–164.

Bellows, Jr, T. S., 1981. The descriptive properties of some models for density dependence. Journal of Animal Ecology 50, 139–156.

Beverton, R. J. H., Holt, S. J., 1956. The theory of fishing. In: Graham, M. (Ed.), Sea Fisheries; Their Investigation in the United Kingdom. Edward Arnold, London, UK, pp. 372–441.

Bier, M., Bountis, T. C., 1984. Remerging Feigenbaum trees in dynamical systems. Physics Letters A 104, 239–244.

Brockwell, P. J., December 1986. The extinction time of a general birth and death process with catastrophes. Journal of Applied Probability 23 (4), 851–858.

Caswell, H., 2001. Matrix Population Models, 2nd Edition. Sinauer, Sunderland, MA.

Caswell, H., Kaye, T. N., 2001. Stochastic demography and conservation of an endangered perennial plant (*Lomatium bradshawii*) in a dynamic fire regime. Advances in Ecological Research 32, 1–51.

Chau, N. P., 2000. Destabilising effect of periodic harvest on population dynamics. Ecological Modelling 127, 1–9.

Clements, F. E., 1916. Plant Succession: An Analysis of the Development of Vegetation. Carnegie Institution of Washington, Washington, DC.

Connell, J. H., March 24 1978. Diversity in tropical rain forests and coral reefs. Science 199 (4335), 1302–1310.

Doebeli, M., 1995. Dispersal and dynamics. Theoretical Population Biology 47, 82–106.

Ernst, A., 1908. The New Flora of the Volcanic Island of Krakatau. Cambridge University Press, Cambridge, UK.

Getz, W. M., 1996. A hypothesis regarding the abruptness of density dependence and the growth rate of populations. Ecology 77 (7), 2014–2026.

Grant, W. E., Pedersen, E. K., Marin, S. L., 1997. Ecology and Natural Resource Management: Systems Analysis and Simulation. John Wiley and Sons.

Grime, J. P., 1973. Competitive exclusion in herbaceous vegitation. Nature 242, 344–347.

Gripenberg, G., 1985. Extinction in a model for the growth of a population subject to catastrophes. Stochastics 14, 149–163.

Hanski, I., 1999. Metapopulation Ecology. Oxford University Press, New York, NY.

Hanson, F. B., Tuckwell, H. C., 1978. Persistence times of populations with large random fluctuations. Theoretical Population Biology 14, 46–61.

Hanson, F. B., Tuckwell, H. C., December 1997. Population growth with randomly distributed jumps. Journal of Mathematical Biology 36 (2), 169–187.

Hassell, M. P., 1975. Density-dependence in single-species populations. Journal of Animal Ecology 44 (1), 283–295.

Hastings, A., Constantino, R. F., July 1987. Cannibalistic egg-larva interactions in *Tribolium*: An explanation for the oscillations in population numbers. American Naturalist 130 (1), 36–52.

Hastwell, G. T., February 2001. On disturbance and diversity: A reply to Mackey and Currie. Oikos 92 (2), 367–371.

Hubbell, S. P., 2001. The Unified Neutral Theory of Biodiversity and Biogeography. No. 32 in Monographs in Population Biology. Princeton University Press, Princeton, NJ.

Huston, M., 1979. A general hypothesis of species diversity. The American Naturalist 113 (1), 81–101.

Hutchinson, G. E., May-June 1961. The paradox of the plankton. American Naturalist 95 (882), 137–145.

Ives, A. R., Gross, K., Jansen, V. A. A., 2000. Periodic mortality events in predator-prey systems. Ecology 81 (12), 3330–3340.

Kaplan, N., Sudbury, A., Nilsen, T. S., 1975. A branching process with disasters. Journal of Applied Probability 12, 47–59.

Lande, R., December 1993. Risks of population extinction from demographic and enviromental stochasticity and random catastrophes. American Naturalist 142 (6), 911–927.

Liu, X., Chen, L., March 2003. Complex dynamics of Holling type II Lotka–Volterra predator–prey system with impulsive perturbations on the predator. Chaos, Solitons, and Fractals 16 (2), 311–320.

Mackey, R. L., Currie, D. J., March 2000. A re-examination of the expected effects of disturbance on diversity. Oikos 88 (3), 483–493.

Maynard Smith, J., Slatkin, M., 1973. The stability of predator-prey systems. Ecology 54, 384–391.

McGlade, J. M., 1999. Individual-based models in ecology. In: McGlade, J. (Ed.), Advanced Ecological Theory : Principles and Applications. Blackwell Science, Malden, MA, pp. 1–22.

Nicholson, A. J., Bailey, V. A., 1935. The balance of animal populations. Proceedings of the Zoological Society of London 3, 551–598.

Pickett, S. T. A., White, P. S. (Eds.), 1985. The Ecology of Natural Disturbance and Patch Dynamics. Academic Press, Orlando, FL.

Ricker, W., 1954. Stock and recruitment. Journal of the Fisheries Research Board of Canada 11, 559–623.

Roberts, M. G., Heesterbeek, J. A. P., 1998. A simple parasite model with complicated dynamics. Journal of Mathematical Biology 37, 272–290.

Rosenzweig, M. L., January 29 1971. Paradox of enrichment: Destabilization of exploitation ecosystems in ecological time. Science 171 (3969), 385–387.

Sheil, D., Burslem, D. F., January 2003. Disturbing hypotheses in tropical forests. Trends in Ecology and Evolution 18 (1), 18–26.

Silva, J. F., Raventos, J., Caswell, H., Trevisan, M. C., June 1991. Population responses to fire in a tropical savanna grass, *Andropogon semiberbis*: A matrix model approach. Journal of Ecology 79 (2), 345–355.

Sommer, U., Worm, B. (Eds.), 2002. Competition and Coexistence. Springer, New York, NY.

Sousa, W. P., 1984. The role of disturbance in natural communities. Annual Review of Ecology and Systematics 15, 353–91.

Southwood, T. R. E., 1976. Bionomic strategies and population parameters. In: May, R. M. (Ed.), Theoretical Ecology: Principles and Applications. W. B. Saunders Company, pp. 26–48.

Stone, L., October 14 1993. Period-doubling reversals and chaos in simple ecological models. Nature 365, 617–620.

Turner, M. G., Romme, W. H., Gardner, R. H., O'Neill, R. V., Kratz, T. K., 1993. A revised concept of landscape equilibrium - disturbance and stability on scaled landscapes. Landscape Ecology 8 (3), 213–227.

Wilkinson, D. M., 1999. The disturbing history of intermediate disturbance. Oikos 84 (1), 145–147.

Wootton, J. T., December 1998. Effects of disturbance on species diversity: A multitrophic perspective. American Naturalist 152 (6), 803–825.

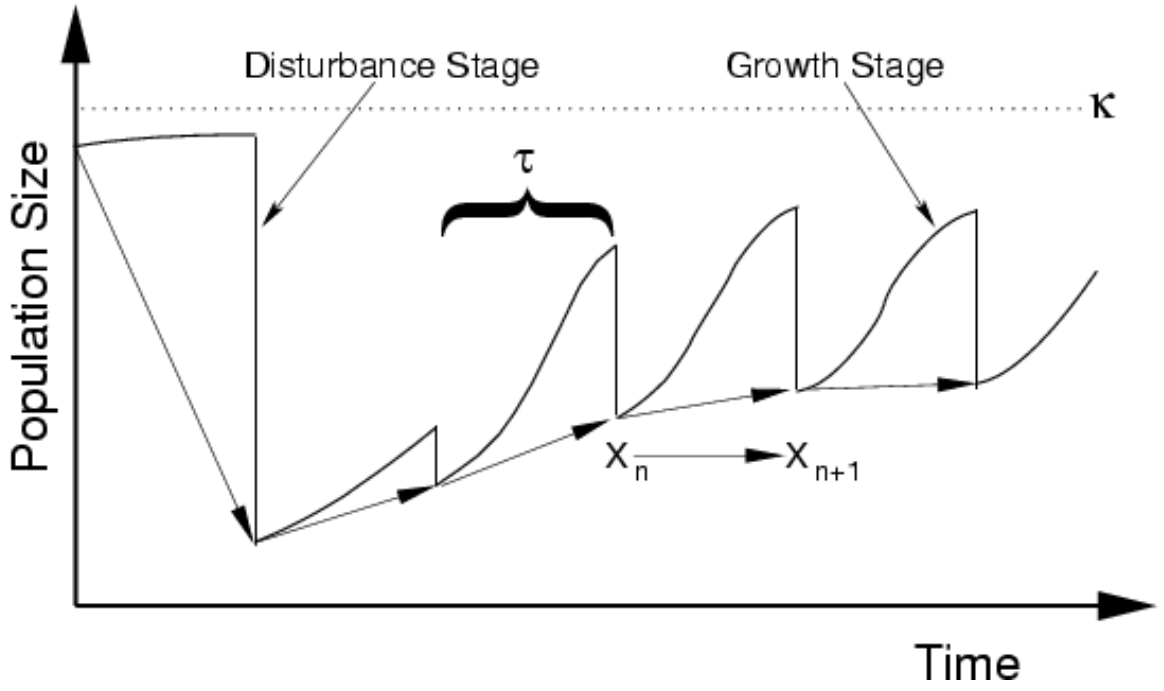

Figure 1: A schematic plot of population dynamics under disturbance. The population size grows toward some carrying capacity κ for some period of time τ before disturbance causes a population crash. The arrows indicate the history of the stroboscopic mapping, which relates the population size after the n'th crash, x_n, to the population size after the $n+1$'th crash, x_{n+1}.

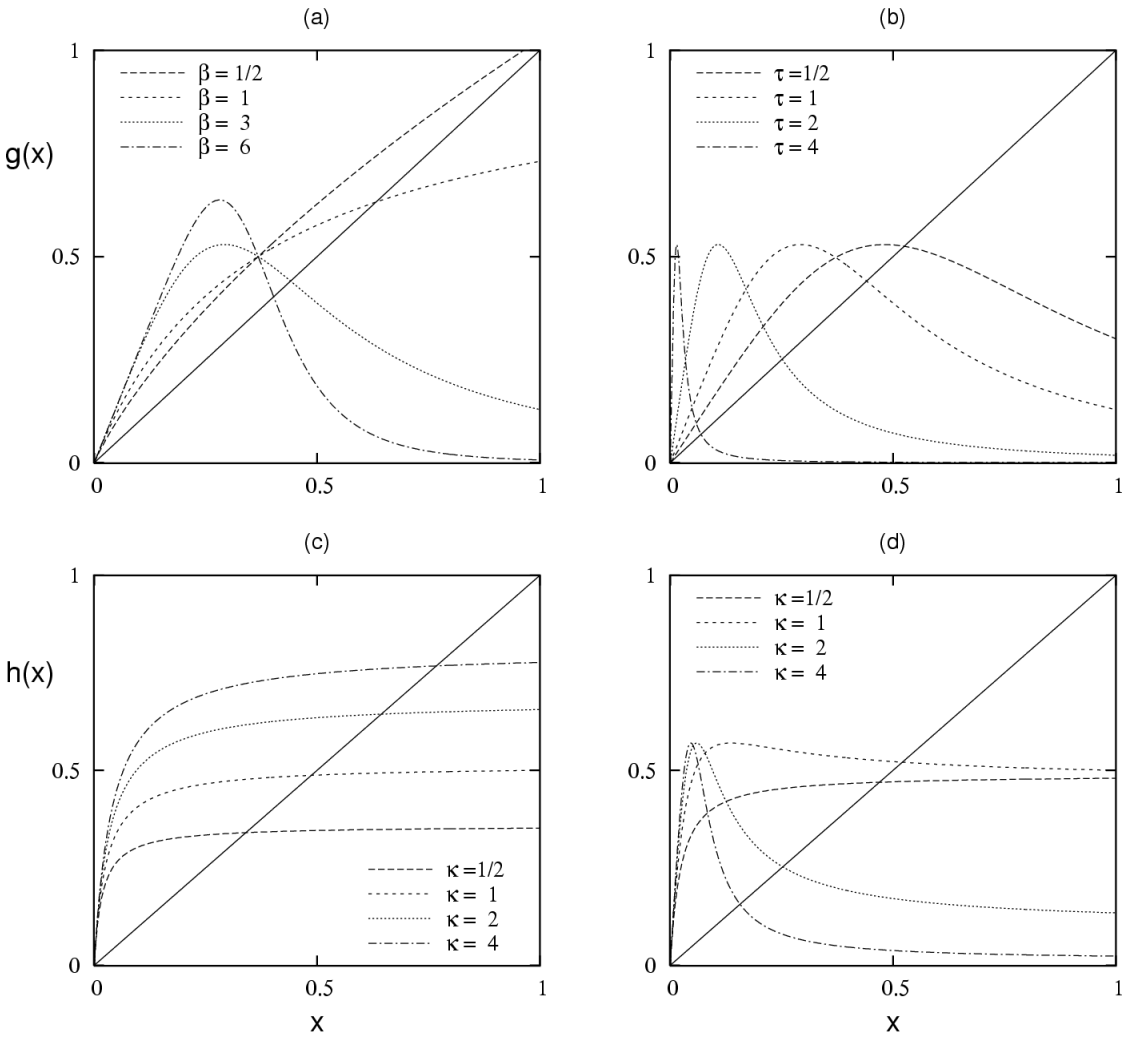

Figure 2: Four diagrams illustrating the shapes of Eqs. (10) and (13): (a) $g(x)$ with $\tau = 1$, (b) $g(x)$ with $\beta = 3$, (c) $h(x)$ with $\beta = 1$ and $\tau = 3$, (d) $h(x)$ with $\beta = 4$ and $\tau = 3$.

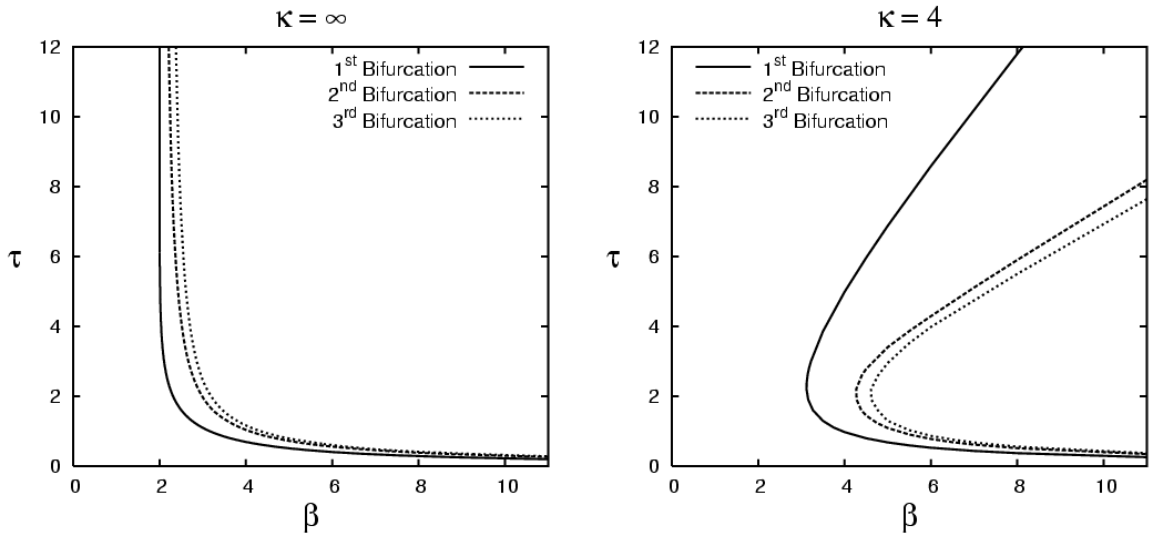

Figure 3: Locations of the first three flip bifurcations of Eq. (13) when $\kappa = \infty$ (left) and $\kappa = 4$ (right). Note that when $\kappa = \infty$, Eq. (13) is equivalent to Eq. (10).

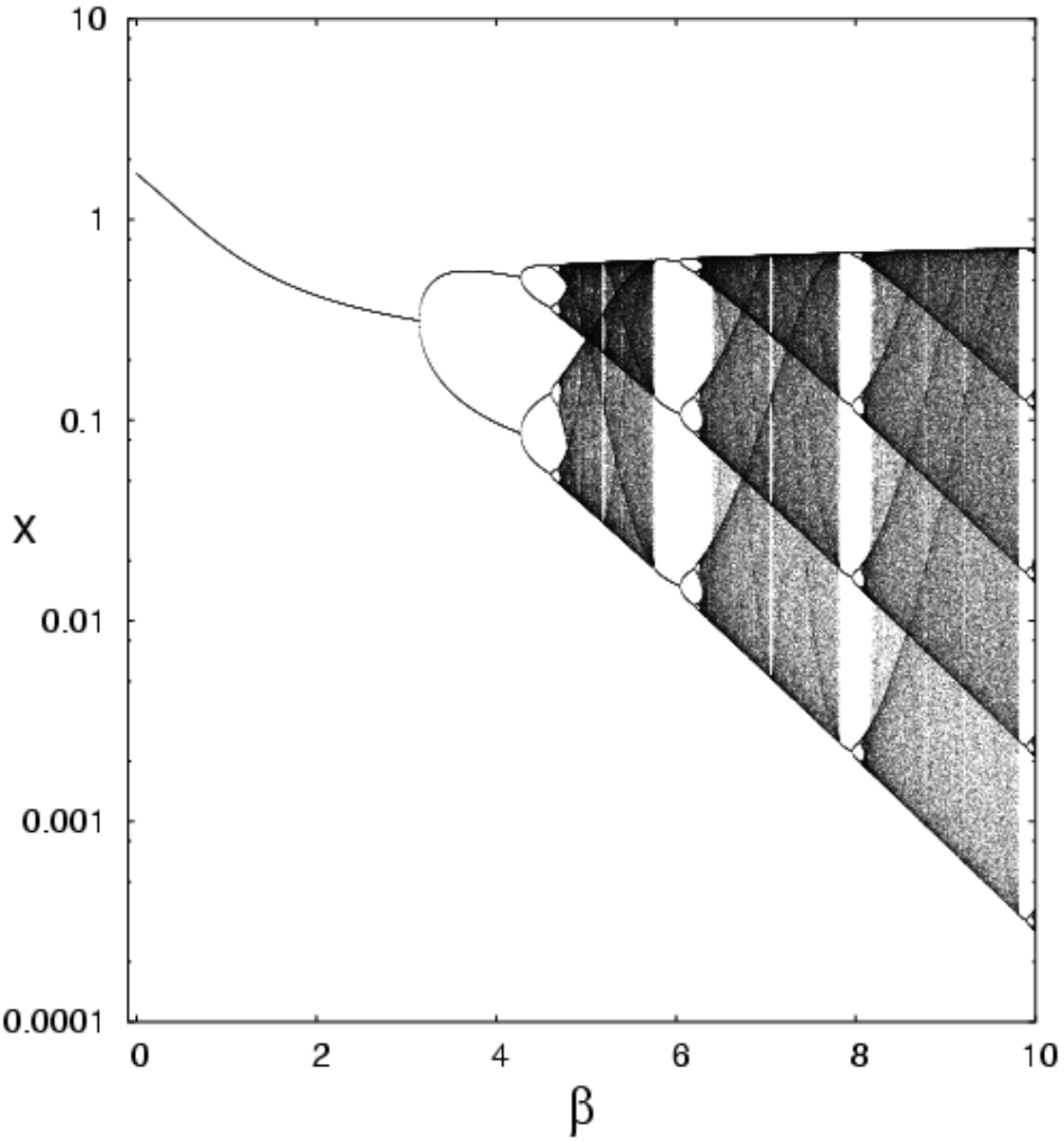

Figure 4: Bifurcation diagram of Eq. (13) in β, with $\tau = 2$ and $\kappa = 4$. For small β, corresponding with weakly nonlinear disturbance, the steady state is stable. As β grows, variability increases, with no abatement. The first 1021 iterations were discarded and 107 points were plotted for each of 3300 β values.

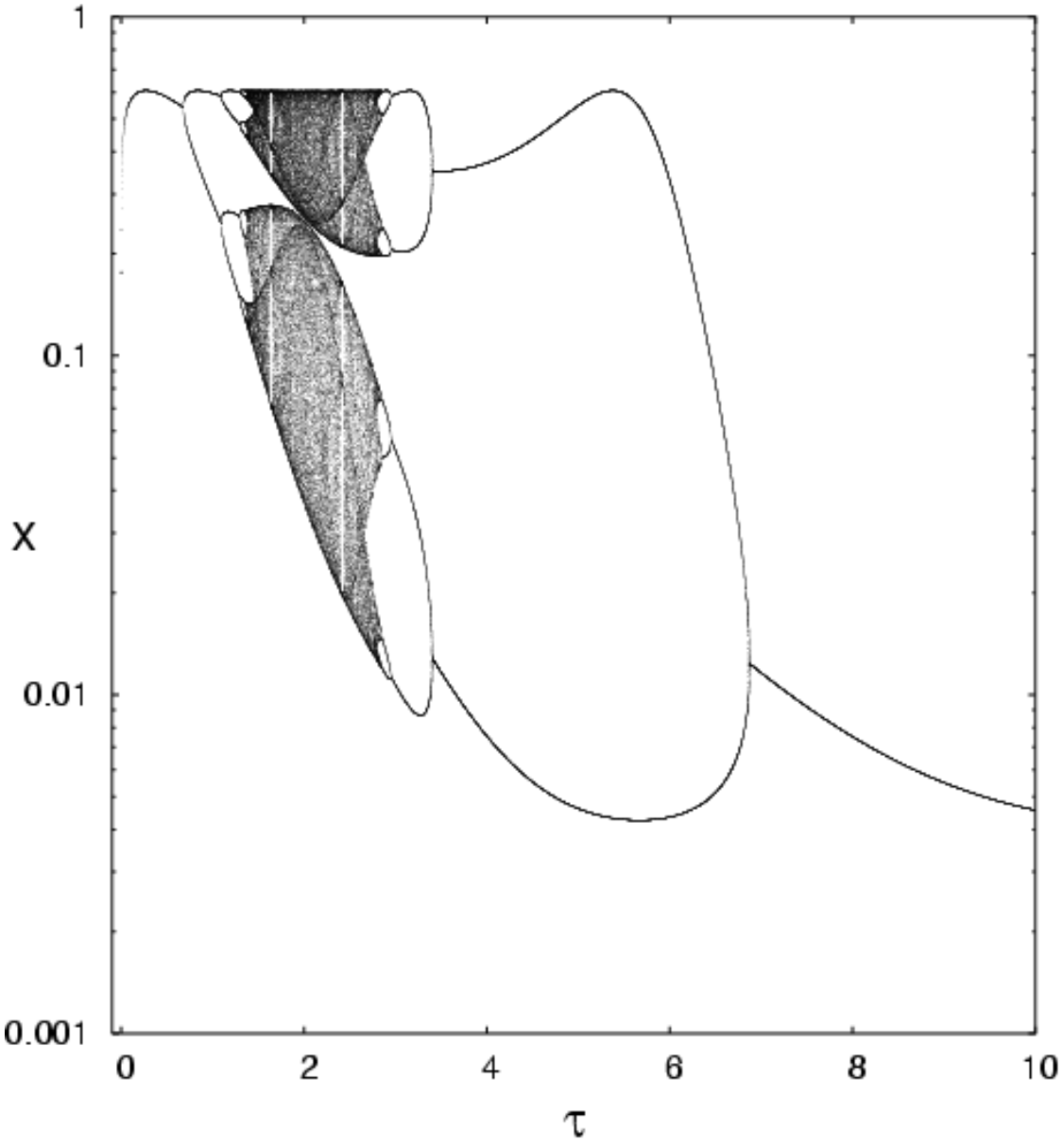

Figure 5: Bifurcation diagram of Eq. (13) in τ, with $\beta = 5$ and $\kappa = 4$. Note the figure can be broken up into four distinct regions of behavior: a boundary layer, a stable regime, a variable regime, and another stable regime. As τ increases, the lowest recurrent population level decays, and the fixed point losses stability before eventually regaining stability. The first 1021 iterations were discarded and 37 points were plotted for each of 30000 τ values.

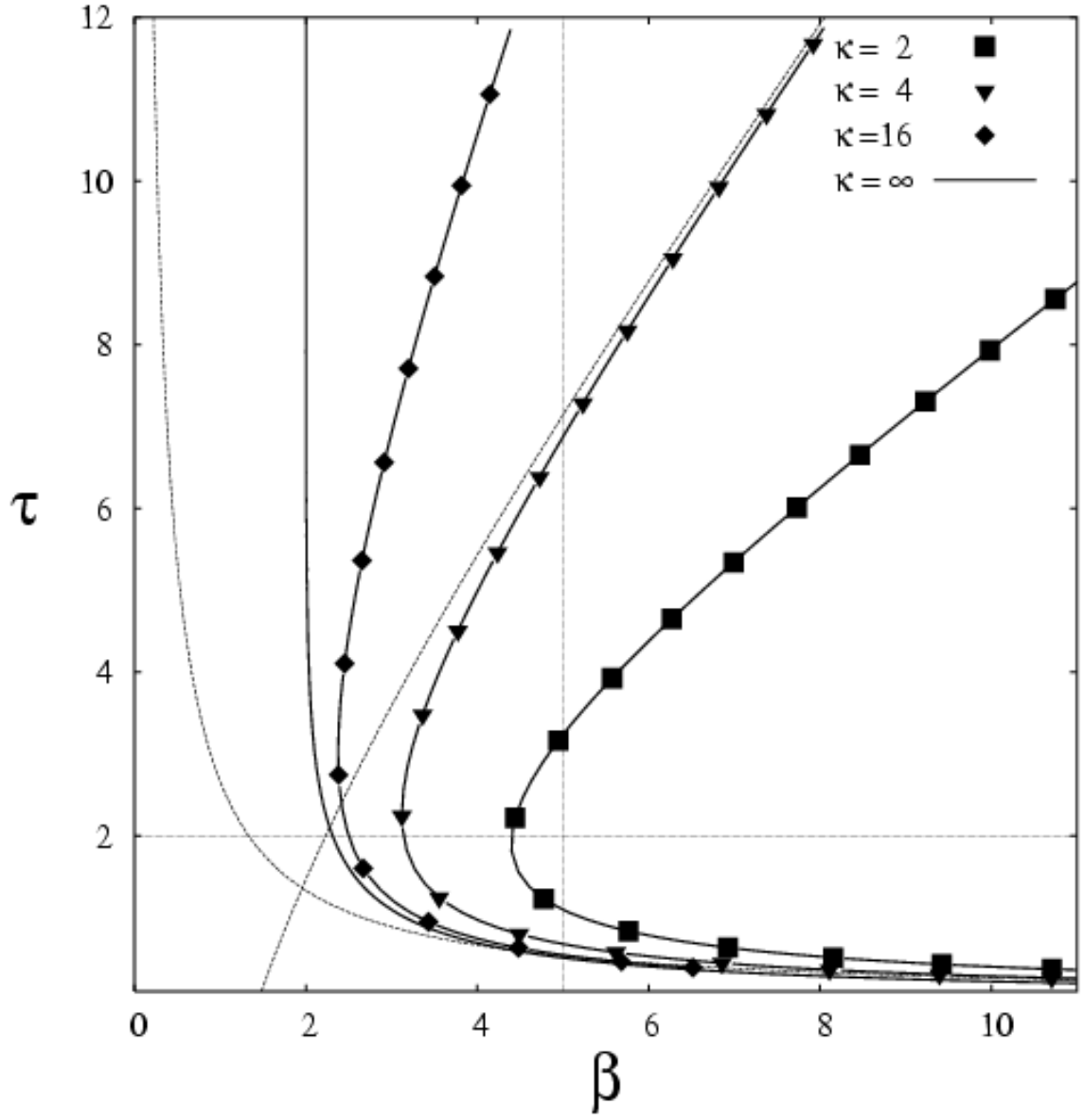

Figure 6: Curves illustrating where in $\tau \times \beta$ parameter space the first flip bifurcation of Eq. (13) occurs for various values of κ. The $\kappa = \infty$ curve corresponds to Eq. (15). The stability regions of the steady state lie to the left of each respective solid curve. The dashed curves are the asymptotic approximations described by Eq. (21) for $\kappa = 4$. The horizontal and vertical dotted lines correspond to the locations of Figs. 4 and 5 respectively.

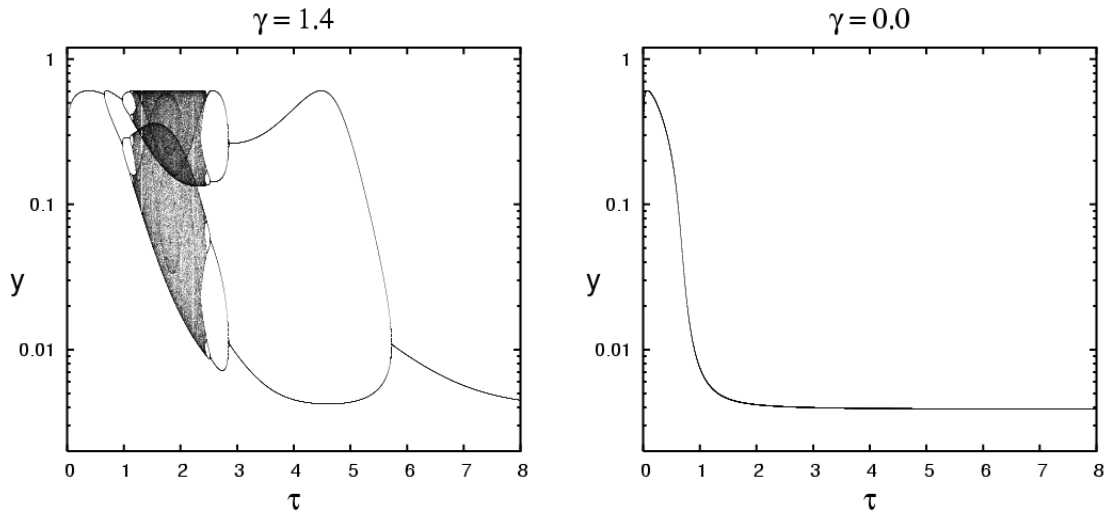

Figure 7: Bifurcation diagram of the seedbank model, Eqs. (34) and (35), with parameters $\beta_1 = \beta_2 = 5$, $\rho = 4$, $\kappa = 4$, $\mu = 1/2$, and $\gamma = 1.4$(left) or $\gamma = 0$(right). Note that there are no observable bifurcations in the case of $\gamma = 0$. Forward and backward bifurcation diagrams have been superimposed. The first 200 iterations were discarded and 60 points were plotted for each of 8000 τ values.